



HHS Public Access

Author manuscript

Curr Biol. Author manuscript; available in PMC 2018 February 06.

Published in final edited form as:

Curr Biol. 2017 February 06; 27(3): 309–317. doi:10.1016/j.cub.2016.11.046.

Environmental geometry aligns the hippocampal map during spatial reorientation

Alex T. Keinath¹, Joshua B. Julian¹, Russell A. Epstein¹, and Isabel A. Muzzio^{2,*}

¹University of Pennsylvania, Department of Psychology, 3710 Hamilton Walk, Philadelphia, Pennsylvania, 19104, USA.

²University of Texas at San Antonio, Department of Biology, 1 UTSA Circle, San Antonio, Texas, 78249, USA.

Summary

When a navigator's internal sense of direction is disrupted, she must rely on external cues to regain her bearings, a process termed spatial reorientation. Extensive research has demonstrated that the geometric shape of the environment exerts powerful control over reorientation behavior, but the neural and cognitive mechanisms underlying this phenomenon are not well understood. Whereas some theories claim that geometry controls behavior through an allocentric mechanism potentially tied to the hippocampus, others postulate that disoriented navigators reach their goals by using an egocentric view-matching strategy. To resolve this debate, we characterized hippocampal representations during reorientation. We first recorded from CA1 cells as disoriented mice foraged in chambers of various shapes. We found that the alignment of the recovered hippocampal map was determined by the geometry of the chamber, but not by nongeometric cues, even when these cues could be used to disambiguate geometric ambiguities. We then recorded hippocampal activity as disoriented mice performed a classical goal-directed spatial memory task in a rectangular chamber. Again, we found that the recovered hippocampal map aligned solely to the chamber geometry. Critically, we also found a strong correspondence between the hippocampal map alignment and the animal's behavior, making it possible to predict the search location of the animal from neural responses on a trial-by-trial basis. Together, these results demonstrate that spatial reorientation involves the alignment of the hippocampal map to local geometry. We hypothesize that geometry may be an especially salient cue for reorientation because it is an inherently stable aspect of the environment.

Graphical Abstract

eTOC Blurb:

*Correspondence should be addressed to I.A.M. (isabel.muzzio@utsa.edu).

Publisher's Disclaimer: This is a PDF file of an unedited manuscript that has been accepted for publication. As a service to our customers we are providing this early version of the manuscript. The manuscript will undergo copyediting, typesetting, and review of the resulting proof before it is published in its final citable form. Please note that during the production process errors may be discovered which could affect the content, and all legal disclaimers that apply to the journal pertain.

Author Contributions: A.T.K., J.B.J., R.A.E., and I.A.M. designed research; A.T.K. and J.B.J. performed research; A.T.K. and J.B.J. analyzed the data; A.T.K., J.B.J., R.A.E., and I.A.M. wrote the paper.

The authors declare no conflict of interest.

Many behavioral studies have shown that lost navigators rely on environmental shape to reorient. Yet the cognitive and neural mechanisms underlying this phenomenon are still debated. Keinath et al. show that, following disorientation, neural activity in the hippocampus orients to the shape of space and this activity predicts reorientation behavior.

Keywords

hippocampus; place cells; cognitive map; spatial reorientation; navigation; geometric module; spatial geometry; disorientation

Introduction

A map, cognitive or otherwise, can be a very useful tool for navigation. It can help a navigator find goals, remember where things are located, and plan novel routes. Yet a map is only effective if the navigator understands where she is on the map and which direction she is facing. Under normal navigating conditions, these internal representations of position and heading can be updated based on self-generated (idiothetic) cues, a process known as path integration [1]. However, on occasion, even the best navigator will become disoriented, in which case their estimates of position and heading will be inaccurate. The navigator must then rely on external (allothetic) cues to regain their bearings—a process known as spatial reorientation.

An extensive behavioral literature suggests that the shape of the local navigable space—the *spatial geometry* of the environment—is an especially powerful cue for reorientation [2,3]. In a now-classic paradigm [4], a disoriented navigator is trained to locate a reward in a corner of a small rectangular chamber. By observing where the navigator subsequently searches for the reward, the cues guiding reorientation can be inferred. Results indicate that navigators search not only at the correct corner, but also the diagonally opposite corner, which is a geometrically equivalent location [4]. Thus, navigators behave as if guided by the spatial geometry of the chamber. Notably, nongeometric cues that could potentially distinguish the geometrically equivalent corners, such as a marking along one wall, are often ignored. This pattern of results—observed across numerous species including birds [5], rodents [4,6], and humans [7]—indicates that reorientation behavior is strongly informed by the spatial geometry of the environment.

These behavioral results are important because they speak to the cognitive mechanisms mediating reorientation [2,3,8–13]. Although any landmark could in theory be used to determine one's heading after disorientation, the strong reliance on geometry suggests that the behavior of the animal is driven by a mechanism that uses global shape parameters of the environment to realign the navigator's cognitive map [4,14,15]. This view remains controversial, however, in part because these results can be alternatively explained without any reference to a cognitive map. Under this competing theory, navigation following disorientation is controlled by an egocentric strategy in which goals are reached by moving to a point where the current visual input matches a stored representation of the visual input at the goal location [16–18]. In this view, “reorientation” primarily involves visual recognition, not the recovery of spatial representations.

Adjudicating between these theories on the basis of behavioral data alone has been difficult, but neural data offer a possible opportunity. Lesion, electrophysiology, and functional neuroimaging studies have demonstrated that allocentric and egocentric navigational strategies are mediated by different neuroanatomical structures. Specifically, allocentric strategies are supported by a neural circuit that includes the hippocampus and neighboring structures, whereas egocentric strategies are mediated by extra-hippocampal circuits [19–24]. Therefore, to test if an allocentric mechanism mediates spatial reorientation, we set out to characterize the hippocampal representations of mice during this process.

Surprisingly, although there is an abundance of research examining hippocampal representations in oriented animals, little is known about how these representations are affected by disorientation. Principal cells in the hippocampus, known as place cells, become active when the navigator occupies a particular location within the environment [21,25]. These location-specific firing fields form a “hippocampal map” that is unique to the navigational context [26]. The hippocampus receives converging inputs from multiple sources and functional cell types [27,28], and under oriented conditions, a mixture of geometric, nongeometric, and idiothetic cues combine to support a reliable, oriented hippocampal map [29–31]. However, the nature of this map following disorientation is less clear. Previous studies examining place cell responses in chambers containing nongeometric cues but without orienting geometry have yielded conflicting results, with some findings suggesting that the hippocampal map is unstable following disorientation [32], and others suggesting that this map is stable and can be oriented by nongeometric cues [33]. Related work examining head direction (HD) cells, whose activity correlates with the alignment of the hippocampal map under oriented conditions, has yielded similar discrepancies in disoriented animals [32,34–37], though some studies suggest a privileged role for spatial geometry [38,39]. Thus, whether the hippocampal map is oriented by geometry following disorientation, and whether this map relates to reorientation behavior, remains unresolved.

If spatial reorientation relies on a mechanism whereby the cognitive map is recovered relative to global shape parameters, then both the hippocampal map and reorientation behavior should be similarly oriented by spatial geometry. If instead spatial reorientation is mediated by an egocentric view-matching mechanism, then the hippocampal map might be unreliable after disorientation or consistently oriented by prominent visual features, with no predictive relationship between the hippocampal map and reorientation behavior. To test these hypotheses, we recorded place cells as disoriented mice repeatedly explored three chambers, each of a different shape and containing an additional distinct visual cue specifying a unique direction within the chamber. We then recorded hippocampal activity as disoriented mice completed the classic spatial reorientation paradigm in a rectangular chamber. To anticipate, we found that a reliable hippocampal map was recovered across trials and that the spatial geometry alone consistently oriented this map; moreover, the orientation of the hippocampal map predicted reorientation behavior on a trial-by-trial basis. Together, these results highlight the role of spatial geometry as a critical cue orienting the hippocampal map and strongly implicate allocentric hippocampal representations as the neural basis of reorientation behavior.

Results

Spatial geometry orients a reliable hippocampal map after disorientation

To assess the potential contributions of spatial geometry and other visual cues to the recovery of the hippocampal map after disorientation, we recorded 48 place cells from dorsal CA1 as 9 mice foraged for randomly scattered chocolate cereal crumbs in a rectangular chamber (Figure 1A). A visual cue that had been previously shown to be discriminable to both oriented and disoriented mice was present along one wall [6]. To disorient the mouse prior to the start of each trial, the mouse was removed from the chamber and placed in a small, lidded cylinder, which was subjected to four full clockwise and counterclockwise rotations. The mouse was then placed back into the chamber facing a random direction. The spatial geometry defined by the walls of the chamber and the polarizing visual cue were the only potential orienting cues available (see Supplemental Experimental Procedures). Mice foraged in this chamber on 12 consecutive testing trials on a single day.

Place cell rate maps illustrating the spatial activity of example place cells recorded from this rectangular chamber are shown in Figure 1B (see also Figure S1A). As illustrated by these rate maps, the place field of each cell either remained at the same location or rotated 180° to the geometrically-equivalent location from trial to trial, in clear contrast to the stability observed in oriented control mice (Figure S1B). This result indicates that the nongeometric cue, which could serve to disambiguate geometrically equivalent facing directions within the chamber, failed to orient the hippocampal map. Rather, chamber geometry alone oriented this map following disorientation.

We quantified this observation by comparing the rate maps of each cell across trials. For each pairwise combination of trials, we first determined the rotation (0°, 90°, 180°, or 270°) that yielded the best match between the two trial rate maps, measured by the pixel-to-pixel cross-correlation. The rectangular rate maps were compressed to squares to make 90° and 270° rotation comparisons possible (Figure 1C). We then calculated the percent of pairwise trial comparisons (66 comparisons for 12 trials) for which each rotation provided the best match, averaging all cells within each animal as the orientations of simultaneously recorded cells may not be independent. The results indicated a striking influence of spatial geometry on the recovered orientation of each cell (Figure 1D). A repeated measures analysis of variance (ANOVA) confirmed that not all rotations yielded the best match equally often ($F(1.6,12.6)=11.1$, $p=0.003$; Greenhouse-Geisser corrected for sphericity violation). Rather, geometrically consistent rotations by 0° or 180° yielded the best match more often than geometrically inconsistent rotations by 90° or 270° (paired t-test: $t(8)=4.0$, $p=0.004$), mirroring the rotational symmetry of the rectangular chamber. Moreover, 0° and 180° yielded the best match equally often (paired t-test: $t(8)=0.9$, $p=0.38$). Similar results were found using an alternative analysis procedure that did not require compression of rate maps, indicating that the effects of spatial geometry are not a product of rate map compression (Figure S1C,D). Together, these results suggest that spatial geometry alone determined the recovered orientations of each cell.

The pronounced influence of spatial geometry on the recovered orientations of individual cells suggests that a reliable hippocampal map is recovered across trials. Indeed, after aligning each map based on the best match rotation, the rate maps of each cell were more similar across trials than expected by chance ($r=0.69\pm 0.01$ mean \pm SEM, $p<0.001$; see Experimental Procedures), and remained highly correlated across trials aligned by both geometrically consistent ($r=0.71\pm 0.02$) and inconsistent ($r=0.64\pm 0.03$) rotations. Notably, the correlations between rate maps aligned by geometrically consistent rotations were significantly higher than the correlations between rate maps aligned by geometrically inconsistent rotations (paired t-test: $t(8)=3.7$, $p=0.006$), suggesting that geometrically inconsistent rotations may reflect a less stable hippocampal map. Simultaneously recorded cells also tended to orient coherently across trials: the patterns of best match rotations were more similar than expected by chance for the majority (77 of 115; 67.0%) of simultaneously recorded cell pairs ($p<0.01$; see Experimental Procedures). Together, these results demonstrate that a reliable and coherent hippocampal map, as observed on similar timescales in oriented mice [40], is recovered following disorientation, and that this map is oriented by spatial geometry.

Given the strong influence of geometry on the recovered orientation of a reliable hippocampal map in a rectangular chamber, we next asked whether similar effects of spatial geometry would be observed in chambers of other shapes. Using the same paradigm, we recorded 66 place cells from dorsal CA1 as 9 disoriented mice repeatedly foraged in a square chamber over 12 consecutive trials (Figure 2A). The square chamber also contained a discriminable visual cue along one wall that uniquely specified orientations within the chamber [6]. Since the square has four-fold rotational symmetry, the use of spatial geometry to orient the hippocampal map should yield four possible map orientations across trials, differing by 90° increments.

Place cell rate maps from this square chamber are shown in Figure 2B (see also Figure S1A). For each cell, we again quantified the percent of pairwise trial comparisons for which each rotation (0° , 90° , 180° , or 270°) provided the best match between rate maps (Figure 2C). A repeated measures ANOVA indicated that the distribution of best match rotations did not differ from chance ($F(2.6,20.8)=2.8$, $p=0.069$; Greenhouse-Geisser corrected), mirroring the rotational symmetry of the chamber. The rate maps of each cell were again more similar across trials after alignment than expected by chance ($r=0.69\pm 0.02$, $p<0.001$). Moreover, the majority (179 of 242; 74.0%) of simultaneously recorded cell pairs oriented coherently across trials ($p<0.01$). Importantly, the similarity of rate maps across trials and the orientation coherence across cells indicate that the distribution of best matching rotations is not the product of random noise. Rather, this distribution reflects four equally likely orientations of a reliable hippocampal map (see also Figure S1D). These results in a square chamber provide further support for the idea that spatial geometry orients the recovered hippocampal map following disorientation.

We then repeated the same procedure in an isosceles triangular chamber (Figure 2D). If the recovered orientation of the hippocampal map is determined by spatial geometry following disorientation, then a single stable orientation should be observed across trials in this chamber, which lacks rotational symmetry. We recorded 37 place cells from dorsal CA1 as 8

disoriented mice repeatedly foraged during 12 consecutive trials. Place cell rate maps from this chamber are shown in Figure 2E (see also Figure S1A). For each cell, we quantified the percent of pairwise trial comparisons for which each rotation (0°, 120°, or 240°) provided the best match between rate maps, first compressing each rate map to an equilateral triangle to make the rotated comparisons possible (Figure 2F). An initial repeated measures ANOVA indicated that not all rotations yielded the best match equally often ($F(1.0,8.3)=30.6$, $p<0.001$; Greenhouse-Geisser corrected). Rather, a rotation by 0° yielded the best match more often than rotations by 120° or 240° (paired t-tests: $t(7)=8.1$, $p<0.001$, and $d\ t(7)=7.7$, $p<0.001$, respectively), consistent with a single stable orientation of a reliable map (see also Figure S1D). Indeed, the rate maps of each cell were more similar across trials than expected by chance even without any additional alignment ($r=0.50\pm 0.04$, $p<0.001$). Thus, as in the rectangular and square, the orientation of the recovered hippocampal map in the triangle is aligned to the chamber geometry.

Taken together, these results indicate that spatial geometry alone consistently orients the hippocampal map following disorientation. To further test this claim, we calculated the Bayes Factor [41,42] comparing the null hypothesis that best match rotations were randomly distributed to the alternative hypothesis that best match rotations were more often consistent with chamber geometry (see Supplemental Experimental Procedures). In the rectangular and triangular chambers, where geometry predicts nonuniform distributions of best match rotations, we found Bayes Factors of 8.97×10^{20} and 1.41×10^{51} respectively, both of which provide very strong evidence in favor of the alternative hypothesis. To verify that nongeometric cues failed to orient the hippocampal map, we compared the null hypothesis that all geometrically consistent rotations were observed with equal frequency to the alternative hypothesis that these rotations were disambiguated by the nongeometric cue. In both the rectangular and square chambers, where multiple orientations are geometrically equivalent, we found Bayes Factors of 1.72 and 0.1 respectively, which together provide evidence in favor of the null hypothesis that nongeometric cues failed to disambiguate geometrically equivalent orientations. Thus, these results provide additional evidence that spatial geometry alone consistently orients the hippocampal map following disorientation.

The recovered orientation of the hippocampal map predicts reorientation behavior on a trial-by-trial basis

We next investigated whether there was a relationship between the recovered orientation of the hippocampal map and reorientation behavior. To this end, we recorded 42 place cells from dorsal CA1 as 7 disoriented mice completed the classic spatial reorientation paradigm, which involves searching for a hidden reward after disorientation. This task thus yielded two potentially related measures of orientation: the orientation of the recovered hippocampal map and the cognitive orientation inferred from search behavior.

The task was conducted in the same rectangular chamber used in the first experiment, except that medicine cups were embedded in the floor near each corner (Figure 3A). These cups were filled with odor-masked bedding at the beginning of each trial, and the cup to the right of the visual cue was consistently rewarded with buried chocolate cereal crumbs. On each trial (12 per day, except for one mouse, who received 8 trials per day) the mouse was

disoriented as previously described and then released in the chamber. The cup in which the mouse first dug for the buried reward was taken as the measure of search behavior. Each trial continued for at least 3 minutes until the mouse found the reward and the chamber was adequately sampled. To ensure that search behavior reflected memory for the reward location and not simply random searching, this task was repeated each day until a performance criterion was met. Data were analyzed only for the first day on which at least 66% of first searches were at the correct or geometric error locations (range 1 to 3 days).

We first confirmed that the pattern of search behavior we observed with this task replicated the typical pattern of reorientation behavior previously characterized with this paradigm [6]. Figure 3A shows the distribution of first search locations for days meeting the performance criterion. As guaranteed by our performance criterion, the majority of first searches were made at either the correct or geometric error locations. Importantly, there was no significant difference in search preference between these two locations (paired t-test: $t(6)=2.0$, $p=0.09$), demonstrating that search behavior was primarily guided by spatial geometry.

Next, we confirmed that spatial geometry also determined the orientation of the recovered hippocampal map during this task, as was the case during free foraging. Figure 3B shows place cell rate maps during this task. For each cell, we again quantified the percent of pairwise trial comparisons for which each rotation (0° , 90° , 180° , or 270°) provided the best match between rate maps (Figure 3C). A repeated measures ANOVA indicated that not all rotations yielded the best match equally often ($F(1.4,8.2)=22.5$, $p=0.002$; Greenhouse-Geisser corrected). Rather, rotations by 0° or 180° yielded the best match more often than rotations by 90° or 270° (paired t-test: $t(6)=4.6$, $p=0.004$; Bayes Factor of 7.14×10^{11} , very strong evidence for geometrically consistent rotations). Furthermore, 0° and 180° yielded the best match equally often (paired t-test: $t(6)=1.5$, $p=0.18$; Bayes Factor of 0.015, evidence for the null hypothesis that geometrically consistent rotations were observed with equal frequency), suggesting that spatial geometry alone determined the recovered orientations of each cell (see also Figure S2A,B). When aligned by their best match rotations, the rate maps of each cell were more similar across trials than would be expected by chance ($r=0.70 \pm 0.02$, $p < 0.001$), and remained highly correlated across trials aligned by both geometrically consistent ($r=0.72 \pm 0.03$) and inconsistent ($r=0.62 \pm 0.05$) rotations, though the difference between these correlations was again significant (paired t-test: $t(6)=3.1$, $p=0.021$). Lastly, the majority (80 of 149; 53.7%) of simultaneously recorded cell pairs were again oriented coherently across trials ($p < 0.01$). These results replicate the pattern we observed in the rectangular chamber during free foraging: the recovered orientation of the hippocampal map is primarily informed by spatial geometry.

Since both the hippocampal map orientation and search behavior were guided by spatial geometry, we next directly addressed the potential relationship between the two. We hypothesized that the orientation of the recovered hippocampal map would predict reorientation behavior on a trial-by-trial basis. Because our performance criterion limited the number of nongeometric errors, we focused the main analyses only on geometrically consistent search trials (see Figure S2C for supplemental analysis of the nongeometric error trials). We first attempted to predict correct and geometric error searches on the basis of the recovered hippocampal map. To do so, we created two average rate maps for each cell, one

of correct searches and one of geometric error searches, by combining all trials during which each behavior was made, excluding the to-be-predicted trial (Figure 3D). We then computed the population vector correlation between the to-be-predicted trial rate maps and the average rate maps derived from correct and geometric error searches, and predicted the behavior corresponding to the higher correlation. Using this method, prediction accuracy for each animal exceeded 50%, with the average prediction accuracy across animals significantly above chance ($80.3\% \pm 4.0\%$; t-test against 50%: $t(6)=7.6$, $p<0.001$; Figure 3E). Moreover, both correct and geometric error trials were reliably predicted (t-test against 50%: $t(6)=6.7$, $p<0.001$, and $t(6)=4.13$, $p=0.006$, respectively), with no significant difference between the prediction accuracy for these two searches (paired t-test: $t(6)=1.0$, $p=0.35$).

We next asked whether the recovered hippocampal map consistently predicted search behavior before the actual search behavior was performed. To do so, we again predicted search behavior on each trial using the average map method, but only included data from incrementally longer time intervals starting from the beginning of the to-be-predicted trial (Figure 3F). This analysis revealed that search behavior could be reliably predicted on the basis of as little as the first 17 s of trial data, earlier than 81.4% of first searches (median time of first search: 32.5 s). Interestingly, during the first 17 s the animals tended to explore the perimeter of the chamber (Figure S2D), suggesting that the animals often had both visual and tactile experience with the chamber geometry prior to making a decision. Moreover, when only data prior to the first search were included for each trial, prediction accuracy remained high ($72.5\% \pm 8.3\%$; $t(6)=2.7$, $p=0.035$). Together, these results demonstrate that reliable and predictive hippocampal maps emerge as early as within the first 17 seconds of the trial, often long before the animal first digs for the reward, suggesting that reorientation is a rapid process.

Finally, we confirmed that the hippocampal maps underlying correct and geometric search behavior were in fact 180° rotations of one another. For each cell, we again created average maps for both behaviors, now including all trials (Figure 3G; see also Figure S2E). Next, we computed the pixel-to-pixel cross-correlation between the average correct map and the 180° -rotated average geometric error map for each cell. We then compared the distribution of these correlation values against a control distribution created by randomly shuffling the average geometric error maps across cells 100 times. Average correct maps were significantly more correlated with the 180° -rotated average geometric error maps than expected by chance (1-sample Kolmogorov-Smirnov test: $D=0.67$, $p<0.001$; Figure 3H). By contrast, average correct maps were not significantly correlated with the unrotated average geometric error maps (1-sample Kolmogorov-Smirnov test: $D=0.15$, $p=0.24$; Figure 3H). Together, these results indicate that the recovered orientation of the hippocampal map, informed by spatial geometry, reliably predicts reorientation search behavior on a trial-by-trial basis.

Discussion

There were two primary results of this study. First, we found that spatial geometry consistently oriented the recovered hippocampal maps of disoriented mice in three differently shaped chambers (rectangle, square, isosceles triangle). From trial to trial, the

orientation of the map varied in a manner that reflected the rotational symmetry of each chamber, despite the presence of nongeometric cues that could potentially disambiguate geometrically equivalent orientations. Second, in a classic reorientation task, we found that the recovered orientation of the hippocampal map predicted goal-directed search behavior on a trial-by-trial basis. These results demonstrate for the first time that spatial geometry is used to realign the hippocampal map after disorientation and that the resulting alignment of the map controls navigational behavior.

These findings have important implications for the ongoing debate over the computations underlying spatial reorientation [2,3,8,9,12–14,18,43]. Allocentric theories claim that reorientation is accomplished by aligning the cognitive map to the surrounding environment to recover one's heading [4,11,13–15]. Egocentric theories, on the other hand, hold that navigation after disorientation reflects the use of a view-matching strategy that does not require heading to be reestablished [16–18]. Our data provide clear evidence for the involvement of the hippocampal map in reorientation, thus supporting the allocentric view. Moreover, the fact that the recovered hippocampal map aligned exclusively to chamber geometry is consistent with the claim that environmental shape plays a privileged role in reorientation. Interestingly, other studies have reported circumstances in which nongeometric cues guide reorientation behavior, such as after oriented, aversive, or extensive experience [32,33,35,44], or when there is a configuration of multiple distal cues [39]; whether the hippocampal map is exclusively aligned by spatial geometry under these other circumstances remains to be tested. However, the fact that we observed a tight correspondence between the geometry of the chamber, the recovered alignment of the hippocampal map, and the search locations of the animals strongly suggests that the reliance on geometry observed in many previous behavioral studies of reorientation is a consequence of the geometric reorientation of the hippocampal map.

At a circuit level, the mechanism by which spatial geometry orients the hippocampal map is currently unknown. This mechanism may involve HD cells, which are active when the navigator faces a particular direction. HD cells are located in a number of regions that interact, directly or indirectly, with the hippocampus, including the medial entorhinal cortex [45], retrosplenial cortex [46], postsubiculum [47], and anterodorsal thalamic nuclei [48]. The preferred directions of HD cells are typically found to be strongly coupled to the alignment of the hippocampal map [32], and spatial geometry is thought to play an important role in determining these preferred directions under disoriented conditions [38,39]. Thus, the hippocampal map may be oriented by HD input in a bottom-up manner [37,49]. Consistent with this view, lesions to the postsubiculum severely impair the recovery of an oriented hippocampal map [50]. On the other hand, lesions to the anterodorsal thalamic nuclei yield comparatively weaker deficits [50], and disjunctions between HD firing in this latter region and reorientation behavior have been reported [36]. Thus, an alternative possibility is that the reorientation signal we observe may instead originate within the hippocampus itself, which in turn updates HD representations in other regions [49].

Because the hippocampal map is often specific to each environment [26], recovery of this map after disorientation must involve more than simply reestablishing heading: the proper map reflecting the current environment must also be recovered. We recently demonstrated

that the processes of identifying the environment and recovering heading after disorientation are behaviorally dissociable, with differential sensitivities to spatial geometry and nongeometric visual cues [6]. Specifically, in a two-chamber reorientation paradigm where disoriented mice were required to both reestablish heading and identify the current chamber, nongeometric visual cues were used for chamber identification but simultaneously ignored for determining heading. Thus, nongeometric cues might play an important role in determining which cognitive map is recovered, even though they are subsequently ignored when reestablishing the alignment of that hippocampal map. Critically, these earlier results suggest that the exclusive alignment of the hippocampal map to chamber geometry observed here does not stem from a failure to notice the nongeometric cues. Rather, spatial geometry plays a unique role in reestablishing heading representations that surpasses mere salience.

In sum, we have shown that a reliable hippocampal map is recovered following disorientation, the orientation of which is determined by the shape of the navigable space. Furthermore, we have shown that the orientation of this map predicts search behavior on a trial-by-trial basis, linking reorientation behavior to allocentric spatial representations. Together, these results provide a critical first step toward understanding the physiological mechanisms that allow navigators to regain their bearings after becoming lost.

Experimental Procedures

Best Match Rotation Analysis

In all experiments, a best match rotation analysis was used to quantify the orientation, reliability, and coherence of the hippocampal map. First, rectangular or isosceles triangular rate maps were compressed to squares or equilateral triangles, respectively. Next, for each cell and each pair of trials, the rotation of the Trial A rate map (square/rectangle: 0°, 90°, 180°, or 270°; triangle: 0°, 120°, 240°) that maximized the pixel-to-pixel correlation to the Trial B rate map was computed. The percent of pairwise trial comparisons for which each rotation yielded the best match was then calculated for each cell. These percentages were then averaged within each animal as the orientations of simultaneously recorded cells are likely not independent.

Rate Map Similarity Analysis

To measure the similarity of rate maps across trials for each cell, the best match rotation correlation value was computed for each pair of trial comparisons, and then averaged across all comparisons. To test significance, these correlation values were averaged across all cells, and this correlation value was compared to a shuffled control generated by randomly shuffling rate maps across cells and trials prior to computing the best match rotations (1000 iterations).

Orientation Coherence Analysis

To measure the orientation coherence of simultaneously recorded cell pairs, the pattern of best match rotations across all pairwise trial comparisons for both cells was compared. The similarity between these patterns was quantified as the proportion of comparisons for which the same rotation yielded the best match. Trial comparisons for which at least one cell in the

pair was inactive were excluded. To assess the significance of this orientation coherence, pattern similarity was compared to a shuffled control created by shuffling the best match rotation pattern order for each cell independently. A cell pair was considered significantly coherent if its similarity exceeded the 99th percentile of 1000 iterations of this shuffled control. Note that this method is overly conservative and thus establishes a lower bound on observed coherence (see also Supplemental Experimental Procedures).

Statistics

All parametric statistical tests are named where appropriate. All t-tests were two-tailed. For a complete description of all Bayes Factors and nonparametric tests see the Supplemental Experimental Procedures.

Supplementary Material

Refer to Web version on PubMed Central for supplementary material.

Acknowledgements

This work was supported by US NIH Grant EY022350, NSF Grants SBE-0541957 and SBE-1041707, NSF CAREER Award 1565410 (I.A.M.), NSF IGERT 0966142 (A.T.K. and J.B.J.), and an NSF Graduate Research Fellowship (J.B.J.).

References

1. Mittelstaedt M-L, Mittelstaedt H. Homing by path integration in a mammal. *Naturwissenschaften*. 1980; 67:566–567.
2. Cheng K, Huttenlocher J, Newcombe NS. 25 years of research on the use of geometry in spatial reorientation: a current theoretical perspective. *Psychon. Bull. Rev.* 2013; 20:1033–54. [PubMed: 23456412]
3. Cheng K, Newcombe NS. Is there a geometric module for spatial orientation? Squaring theory and evidence. *Psychon. Bull. Rev.* 2005; 12:1–23. [PubMed: 15945200]
4. Cheng K. A purely geometric module in the rat's spatial representation. *Cognition*. 1986; 23:149–78. [PubMed: 3742991]
5. Lee SA, Spelke ES, Vallortigara G. Chicks, like children, spontaneously reorient by three-dimensional environmental geometry, not by image matching. *Biol. Lett.* 2012; 8:492–4. [PubMed: 22417791]
6. Julian JB, Keinath AT, Muzzio IA, Epstein RA. Place recognition and heading retrieval are mediated by dissociable cognitive systems in mice. *Proc. Natl. Acad. Sci.* 2015; 112:6503–6508. [PubMed: 25941390]
7. Hermer L, Spelke ES. A geometric process for spatial reorientation in young children. *Nature*. 1994; 370:57–9. [PubMed: 8015605]
8. Wang R, Spelke E. Human spatial representation: insights from animals. *Trends Cogn. Sci.* 2002; 6:376. [PubMed: 12200179]
9. Lee SA, Spelke ES. Two systems of spatial representation underlying navigation. *Exp. brain Res.* 2010; 206:179–88. [PubMed: 20614214]
10. Burgess N. Spatial memory: how egocentric and allocentric combine. *Trends Cogn. Sci.* 2006; 10:551–7. [PubMed: 17071127]
11. Miller NY, Shettleworth SJ. Learning about environmental geometry: an associative model. *J. Exp. Psychol. Anim. Behav. Process.* 2007; 33:191–212. [PubMed: 17620021]

12. Sheynikhovich D, Chavarriaga R, Strösslin T, Arleo A, Gerstner W. Is there a geometric module for spatial orientation? Insights from a rodent navigation model. *Psychol. Rev.* 2009; 116:540–66. [PubMed: 19618986]
13. Learmonth AE, Newcombe NS, Sheridan N, Jones M. Why size counts: children's spatial reorientation in large and small enclosures. *Dev. Sci.* 2008; 11:414–26. [PubMed: 18466375]
14. Gallistel, CR. *The organization of learning.* Bradford Books/MIT Press; Cambridge, MA: 1990.
15. Doeller CF, King JA, Burgess N. Parallel striatal and hippocampal systems for landmarks and boundaries in spatial memory. *Proc. Natl. Acad. Sci. U. S. A.* 2008; 105:5915–20. [PubMed: 18408152]
16. Zeil J, Hofmann MI, Chahl JS. Catchment areas of panoramic snapshots in outdoor scenes. *J. Opt. Soc. Am. A. Opt. Image Sci. Vis.* 2003; 20:450–69. [PubMed: 12630831]
17. Pecchia T, Vallortigara G. View-based strategy for reorientation by geometry. *J. Exp. Biol.* 2010; 213:2987–96. [PubMed: 20709927]
18. Stürzl W, Cheung A, Cheng K, Zeil J. The information content of panoramic images I: The rotational errors and the similarity of views in rectangular experimental arenas. *J. Exp. Psychol. Anim. Behav. Process.* 2008; 34:1–14. [PubMed: 18248111]
19. Packard MG, McGaugh JL. Inactivation of hippocampus or caudate nucleus with lidocaine differentially affects expression of place and response learning. *Neurobiol. Learn. Mem.* 1996; 65:65–72. [PubMed: 8673408]
20. Packard MG, McGaugh JL. Double dissociation of fornix and caudate nucleus lesions on acquisition of two water maze tasks: further evidence for multiple memory systems. *Behav. Neurosci.* 1992; 106:439–46. [PubMed: 1616610]
21. O'Keefe, J., Nadel, L. *The Hippocampus as a Cognitive Map.* Oxford University Press; 1978.
22. Barnes TD, Kubota Y, Hu D, Jin DZ, Graybiel AM. Activity of striatal neurons reflects dynamic encoding and recoding of procedural memories. *Nature.* 2005; 437:1158–61. [PubMed: 16237445]
23. Iaria G, Petrides M, Dagher A, Pike B, Bohbot VD. Cognitive strategies dependent on the hippocampus and caudate nucleus in human navigation: variability and change with practice. *J. Neurosci.* 2003; 23:5945–52. [PubMed: 12843299]
24. Maguire EA, Burgess N, Donnett JG, Frackowiak RS, Frith CD, O'Keefe J. Knowing where and getting there: a human navigation network. *Science.* 1998; 280:921–4. [PubMed: 9572740]
25. O'Keefe J. Place units in the hippocampus of the freely moving rat. *Exp. Neurol.* 1976; 51:78–109. [PubMed: 1261644]
26. Alme CB, Miao C, Jezek K, Treves A, Moser EI, Moser M-B. Place cells in the hippocampus: eleven maps for eleven rooms. *Proc. Natl. Acad. Sci. U. S. A.* 2014; 111:18428–35. [PubMed: 25489089]
27. Zhang S-J, Ye J, Miao C, Tsao A, Cerniauskas I, Ledergerber D, Moser M-B, Moser EI. Optogenetic dissection of entorhinal-hippocampal functional connectivity. *Science.* 2013; 340:1232627. [PubMed: 23559255]
28. Witter MP, Groenewegen HJ, Lopes da Silva FH, Lohman AH. Functional organization of the extrinsic and intrinsic circuitry of the parahippocampal region. *Prog. Neurobiol.* 1989; 33:161–253. [PubMed: 2682783]
29. Muller RU, Kubie JL. The effects of changes in the environment on the spatial firing of hippocampal complex-spike cells. *J. Neurosci.* 1987; 7:1951–68. [PubMed: 3612226]
30. O'Keefe J, Speakman A. Single unit activity in the rat hippocampus during a spatial memory task. *Exp. brain Res.* 1987; 68:1–27. [PubMed: 3691688]
31. Jeffery KJ, Donnett JG, Burgess N, O'Keefe JM. Directional control of hippocampal place fields. *Exp. brain Res.* 1997; 117:131–42. [PubMed: 9386011]
32. Knierim JJ, Kudrimoti HS, McNaughton BL. Place cells, head direction cells, and the learning of landmark stability. *J. Neurosci.* 1995; 15:1648–59. [PubMed: 7891125]
33. Dudchenko PA, Goodridge JP, Taube JS. The effects of disorientation on visual landmark control of head direction cell orientation. *Exp. Brain Res.* 1997; 115:375–80. [PubMed: 9224866]

34. Taube JS, Muller RU, Ranck JB. Head-direction cells recorded from the postsubiculum in freely moving rats. II. Effects of environmental manipulations. *J. Neurosci.* 1990; 10:436–447. [PubMed: 2303852]
35. Clark BJ, Taube JS. Intact landmark control and angular path integration by head direction cells in the anterodorsal thalamus after lesions of the medial entorhinal cortex. *Hippocampus.* 2011; 21:767–82. [PubMed: 21049489]
36. Golob EJ, Stackman RW, Wong AC, Taube JS. On the behavioral significance of head direction cells: neural and behavioral dynamics during spatial memory tasks. *Behav. Neurosci.* 2001; 115:285–304. [PubMed: 11345955]
37. Golob EJ, Taube JS. Head direction cells and episodic spatial information in rats without a hippocampus. *Proc. Natl. Acad. Sci. U. S. A.* 1997; 94:7645–50. [PubMed: 9207146]
38. Knight R, Hayman R, Lin Ginzberg L, Jeffery K. Geometric cues influence head direction cells only weakly in nondisoriented rats. *J. Neurosci.* 2011; 31:15681–92. [PubMed: 22049411]
39. Clark BJ, Harris MJ, Taube JS. Control of anterodorsal thalamic head direction cells by environmental boundaries: comparison with conflicting distal landmarks. *Hippocampus.* 2012; 22:172–87. [PubMed: 21080407]
40. Kentros CG, Agnihotri NT, Streater S, Hawkins RD, Kandel ER. Increased attention to spatial context increases both place field stability and spatial memory. *Neuron.* 2004; 42:283–95. [PubMed: 15091343]
41. Gallistel CR. The importance of proving the null. *Psychol. Rev.* 2009; 116:439–453. [PubMed: 19348549]
42. Dienes Z. Bayesian Versus Orthodox Statistics: Which Side Are You On? *Perspect. Psychol. Sci.* 2011; 6:274–90. [PubMed: 26168518]
43. Spelke ES, Kinzler KD. Core knowledge. *Dev. Sci.* 2007; 10:89–96. [PubMed: 17181705]
44. Golob EJ, Taube JS. Differences between appetitive and aversive reinforcement on reorientation in a spatial working memory task. *Behav. Brain Res.* 2002; 136:309–16. [PubMed: 12385817]
45. Sargolini F, Fyhn M, Hafting T, McNaughton BL, Witter MP, Moser M-B, Moser EI. Conjunctive representation of position, direction, and velocity in entorhinal cortex. *Science.* 2006; 312:758–62. [PubMed: 16675704]
46. Chen LL, Lin LH, Green EJ, Barnes CA, McNaughton BL. Head-direction cells in the rat posterior cortex. I. Anatomical distribution and behavioral modulation. *Exp. brain Res.* 1994; 101:8–23. [PubMed: 7843305]
47. Taube JS, Muller RU, Ranck JB. Head-direction cells recorded from the postsubiculum in freely moving rats. I. Description and quantitative analysis. *J. Neurosci.* 1990; 10:420–35. [PubMed: 2303851]
48. Taube JS. Head direction cells recorded in the anterior thalamic nuclei of freely moving rats. *J. Neurosci.* 1995; 15:70–86. [PubMed: 7823153]
49. Golob EJ, Taube JS. Head direction cells in rats with hippocampal or overlying neocortical lesions: evidence for impaired angular path integration. *J. Neurosci.* 1999; 19:7198–7211. [PubMed: 10436073]
50. Calton JL, Stackman RW, Goodridge JP, Archey WB, Dudchenko PA, Taube JS. Hippocampal place cell instability after lesions of the head direction cell network. *J. Neurosci.* 2003; 23:9719–31. [PubMed: 14585999]

Highlights

- Spatial geometry orients the hippocampal map recovered following disorientation
- Hippocampal map orientation predicts reorientation behavior

Author Manuscript

Author Manuscript

Author Manuscript

Author Manuscript

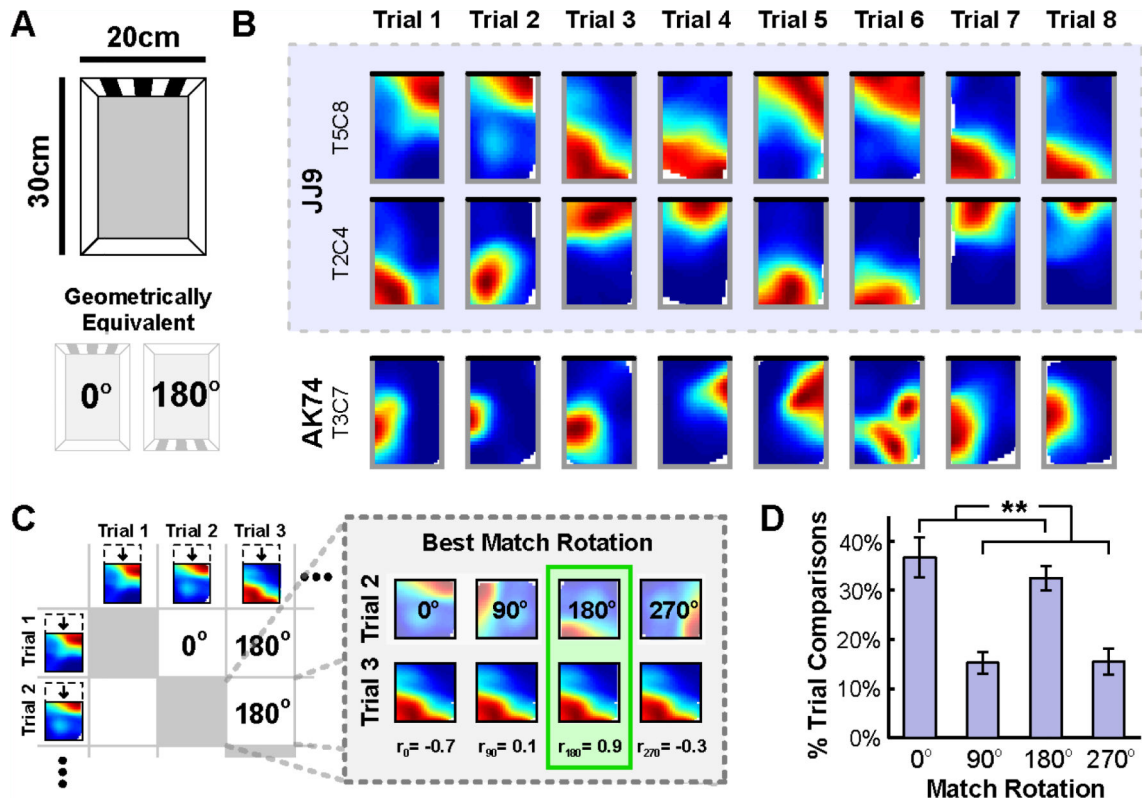


Figure 1. Spatial geometry orients a reliable hippocampal map following disorientation in a rectangular chamber

A) Schematic of the rectangular chamber and the polarizing visual cue. Note that two rotations of this chamber, 0° and 180°, result in geometrically equivalent shapes. B) Example rate maps from the first 8 trials for three place cells, two of which were simultaneously recorded (blue shading). Black line indicates the location of the visual cue. C) Quantification of best match rotations. To quantify the orientation of rate maps across trials for each place cell, the rotation that yielded the best match (highest correlation) between the two rate maps for each pair of trials was determined. D) Distribution of best match rotations across animals, computed as the percent of pairwise trial comparisons for which each rotation yielded the best match. The 0° and 180° rotations most often and equally often yielded the best match, mirroring the rotational symmetry of the rectangular chamber. All error bars denote ± 1 standard error of the mean (SEM) across animals. See also Figure S1. ** $p < 0.01$

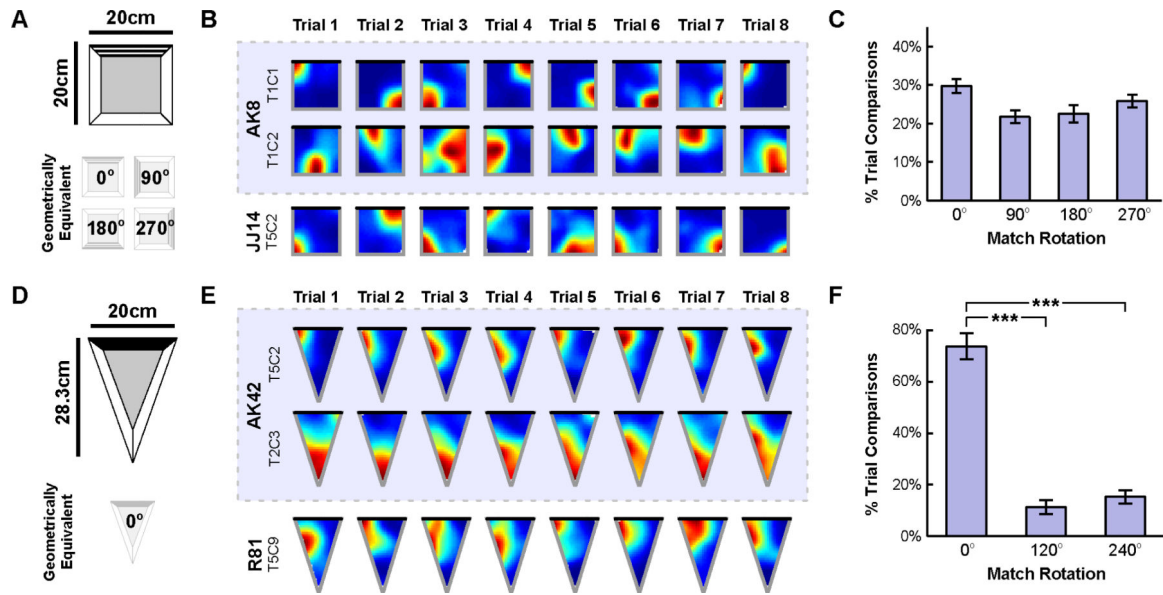


Figure 2. Spatial geometry orients a reliable hippocampal map following disorientation in a square and isosceles triangular chamber

A) Schematic of the square chamber and the polarizing visual cue. Note that four rotations of the square chamber, 0° , 90° , 180° , and 270° , result in geometrically equivalent shapes. B) Example rate maps from the first 8 trials in the square chamber for three place cells, two of which were simultaneously recorded (blue shading). Black line indicates the location of the visual cue. C) Distribution of best match rotations across animals in the square chamber. This distribution did not differ from chance, mirroring the rotational symmetry of the square chamber. D) Schematic of the isosceles triangular chamber and the polarizing visual cue. Note that this chamber lacks rotational symmetry. E) Example rate maps from the first 8 trials in the triangular chamber for three place cells, two of which were simultaneously recorded (blue shading). Black line indicates the location of the visual cue. F) Distribution of best match rotations across animals in the triangular chamber. Only a rotation of 0° yielded the best match more often than chance, mirroring the lack of rotational symmetry of this chamber. All error bars denote ± 1 SEM across animals. See also Figure S1. *** $p < 0.001$

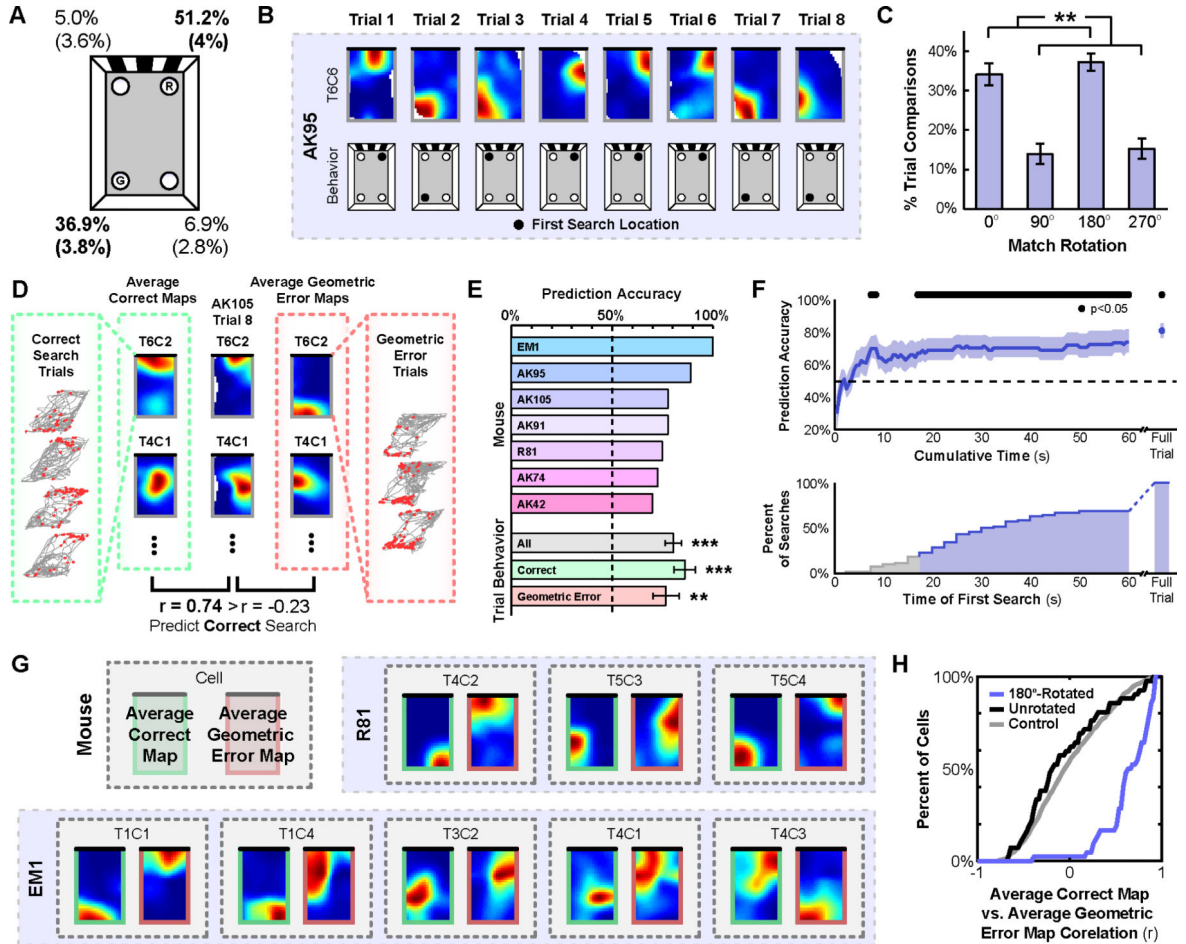


Figure 3. The orientation of the recovered hippocampal map predicts search behavior during a spatial reorientation task on a trial-by-trial basis

A) Schematic of the chamber with the rewarded (R) and geometric error (G) locations noted, and the corresponding distribution of first searches (mean \pm (SEM)). B) Examples of place cell rate maps and search behavior from the first 8 trials during the spatial reorientation paradigm. C) Distribution of best match rotations across animals during the spatial reorientation paradigm. Rotations of 0° and 180° most often and equally often yielded the best match, mirroring the rotational symmetry of the chamber. D) Schematic of the behavior prediction analysis. To predict behavior on each trial, two average maps were created by combining either all other correct or all other geometric error search trials for each cell. Then, the population vector correlation between the to-be-predicted trial rate maps and each of the average behavior rate maps were calculated, and the behavior corresponding to the higher correlation was predicted. E) Individual and average prediction accuracy. F) Prediction accuracy using only data from cumulatively longer time intervals starting from the beginning of the to-be-predicted trial (top), and the cumulative distribution of the time of first search (bottom). G) Example average behavior rate maps, including all trials with the corresponding behavior. H) Cumulative distributions of correlations between the average correct map and the average geometric error map, either rotated 180° or unrotated, compared

to a shuffled control. All error bars denote ± 1 SEM across animals. See also Figure S2.
** $p < 0.01$; *** $p < 0.001$

Author Manuscript

Author Manuscript

Author Manuscript

Author Manuscript